Article

Performance Analysis of a Compact Conformal SWB Antenna for 5G and Wearable IoT Applications

Dipika Sagne[1], Rashmi A. Pandhare[1]
[1] *Department of Electronics & Communication Engineering, Indian Institute of Information Technology, Nagpur, India. deepika.sagne@gmail.com, rush9ap@gmail.com*

***Abstract*— This paper focused on the design and practical implementation of a compact arrowhead slot Super Wide Band (SWB) antenna on a semi-flexible substrate for a wide range of applications. A tapered feed circular monopole antenna with an arrowhead-shaped slot structure is designed on RT/Duroid substrate with a compact physical dimension of 22 × 28 × 0.508 mm3. The impedance bandwidth of the proposed antenna is 95.93 GHz (3.1- 99.17 GHz) with a peak gain of 6.91 dBi. The proposed antenna has a fractional bandwidth of 187% with a high Bandwidth Dimension Ratio (BDR) of 3049 which makes the proposed antenna suitable for a wide range of applications. The proposed antenna compactness is theoretically verified with the help of the fundamental dimension limit theorem. For wearable IoT applications compactness, conformal and bending capabilities of materials are essential and hence the proposed antenna is also tested under different bending conditions and achieved a minor effect on the antenna performance. Further in order to observe the signal correlation, the time domain analysis using similar antennas in face-to-face and side-to-side scenarios has been also analyzed. The simulated results of the proposed antenna exhibit good agreement with the experimental results of the prototype model antenna.**

Index Terms— BDR, Conformal, Fundamental dimension limit theorem, SWB.

I. INTRODUCTION

Many countries are on the verge of deploying the fifth generation mobile network. This 5G technology would employ the existing fourth Generation (4G) band as well as newly defined fifth Generation (5G) frequency ranges, which would include millimeter wave (mm Wave) bands (26, 28, 40, 50, and 66 GHz) [1]–[4]. The Internet of Things (IoT), on the other hand, is a rapidly emerging technology that aims to transform and seamlessly connect the world through various smart devices. Wearable devices of various types are predicted and assumed to be an important part of the IoT. These IoT devices require an increased data rate to operate, and this 5G technology has an imperative role to play in the domain of Internet of Things applications to provide a high data rate to operate on. Due to the recent developments in wireless technology, the next-generation communication systems demand a compact, low-cost, lightweight, efficient, low-power, portable, and accessible

  ISSN 2179-1074

antenna that can provide integration flexibility and work with high data rates and high-quality wireless connectivity that can easily maintain reliable and high-performance communication for both short and long-distance [5].

The use of Ultra Wide-Band (UWB) radio technology can meet the need for high data rate wireless communication over short distances [6], [7]. However, for long-range communication, when a single antenna is used for various communication systems in a single portable device for long-range data transfers, UWB technology may not be sufficient. In this scenario, a Super Wide-Band (SWB) antenna, stands as a promising solution and provides ubiquitous coverage by covering both short and long-range transmissions [8].

In order to fulfil the demanding requirements of modern wireless communication systems and to incorporate the advantages of SWB technology, several design techniques have been reported in the literature. Antenna designers have proposed changes to the ground structure and patch techniques with the help of chamfering and blending, as well as different types of feeding techniques [9]–[14] and Coplanar Waveguide (CPW) [15]–[18] feeding. The self-similarity structures [19]–[21] have been reported by many researchers in the literature for enhancement of bandwidth. The super wide bandwidth by deploying a fusion of elliptical patch geometries with a semi-elliptical ground plane, loaded with a V-cut at the ground, is reported in [9]. The antenna is suitable for super ultra wideband (UWB) upper wide impedance bandwidth from 1.9 GHz to a frequency of over 30 GHz. In [10], a compact offset elliptical ring microstrip patch antenna with an impedance bandwidth of (2.31–40.0 GHz) for SWB applications is described. A tapered microstrip feed line is used in this work as it offers a wider impedance bandwidth with a smoother current path. In [11] describe patch's modified structure, which includes a 50-Ω tapered feed line and engraving slots on the ground plane and provides a wider impedance bandwidth (3 to 50 GHz) as well as lower cross-polarized and omnidirectional radiation patterns. Using patch and ground modification in [12], as well as tapered feed line and bending techniques, describe a compact, high bandwidth (2.3 to 34.8 GHz) dimension ratio steering shaped super wideband antenna for future wireless communication applications. In [13], [14], a super wide band antenna with modifications in the ground structure and patch with the assistance of chamfering techniques has been reported. In [15] it presents a super-wideband antenna based on a propeller-shaped printed monopole with a CPW feed with a wide impedance bandwidth from 3 to 35 GHz with a gain of 4 dBi to 5.2 dBi. In [16], a CPW-fed super-wideband antenna with a modified vertical bow-tie-shaped patch for wireless sensor networks is presented with a peak gain of 4.56 dBi and an average efficiency of 76.62%. In [17], a CPW-fed small bulb-shaped planar super wideband (SWB) antenna operating over the 2.8–40 GHz spectrum is proposed. The antenna offers a fractional bandwidth of 173.8%, a bandwidth dimension ratio (BDR) of 1904, a measured peak gain of 5.5 dBi, and a radiation efficiency of 80%. The reflective FSS layer at an optimal air gap of 8 mm is reported in this work to improve the gain of an antenna. [18] Described a compact co-planar waveguide (CPW)-fed circular monopole super ultra-wideband (UWB) antenna with a frequency

  ISSN 2179-1074

band from 3.1 to more than 20 GHz. The antenna provides a monopole like radiation pattern with a high radiation efficiency of more than 80% and flat gain variation between 2 and 5 dBi. A hexagonal-shaped fractal antenna with a triangular slot for super wideband (SWB) application is presented in [19]. The proposed antenna is made up of triangular slots on a hexagonal metallic patch with a tapered microstrip line feed and a bandwidth ranging from 3 to 35 GHz. [20] describes the SWB antenna with an inscribed fractal structure with a tapered feed line and partial ground plane with blended corners and achieves a super wideband frequency range from 2.31 GHz to 105.5 GHz. In [21], a staircase fractal curve is applied to a microstrip line fed truncated corner square patch antenna to achieve Super Wide Band (SWB) operation with an impedance bandwidth from 0.1 GHz to 30 GHz.

The SWB antennas that have recently been developed are suitable for a wide range of wireless applications. However, due to recent advancements in the field of modern wireless communication systems, the growing popularity of commercial wearable gadgets has piqued the interest of several research advancements in the field of wearable sensing technologies. The upcoming Internet of Things (IoT) era is reshaping how gadgets connect with wearable devices, which include wearable electronics with flexible antennas [22]. As a result, flexible antennas have received a lot of attention in this context, and hence further research has been conducted on the flexibility and seamless integrity of the SWB flexible antennas. [23] Describes a small-sized, low-profile, planar, and flexible ultra-wide band (UWB) antenna made of natural rubber as the substrate. The antenna operates from 3.1–10.6 GHz and the parameters such as return loss, VSWR, radiation pattern, radiation efficiency, and peak gain are analyzed. In [24], a compact SWB antenna is designed on a thin and flexible ultralam 3850 laminate with a physical dimension of 60×40×0.1 mm^3, and it uses a circular disc monopole structure. The designed antenna is thoroughly analyzed in terms of its reflection coefficient, radiation pattern, gain, radiation efficiency, and surface current. In [25], a flexible monopole UWB antenna is fabricated on a paper substrate with a physical dimension of 33.1×32.7×0.254 mm^3 for IoT wearable applications. However, bending and time domain analyses were not performed in any of the above-mentioned papers. [26] Presents a flexible antenna implemented on a PET substrate for 5G applications with total dimensions of 60 x 75 mm^2 fabricated using a novel inkjet printer and silver nanoparticles as the conductive ink. The antenna operates within the 7 to 13 GHz band with an average gain of 5 dBi. The flexible antenna was also tested under bending conditions. On the other hand, the size of the antenna is much larger compared to a lower resonating frequency. In [27], a novel flexible broadband antenna including the CPW feed line with a physical dimension of 92 × 121.5 × 2 mm^3 is reported for IoT applications. The effects of bending on the antenna performance have also been investigated in this work. However, the antenna has an impedance bandwidth of 0.856–2.513 GHz only, which makes the proposed antenna suitable only for short-distance communication and the antenna size is also very large. Based on the literature review, it was discovered that combining work on a compact super wideband flexible antenna with bending and time domain analysis for wearable IoT applications has yet to be reported.

Brazilian Microwave and Optoelectronics Society-SBMO *received 27 Sep 2023; for review 11 Dec 2023; accepted 23 May 2024*
Brazilian Society of Electromagnetism-SBMag *ISSN 2179-1074*

A tapered circular shaped monopole antenna with an arrowhead shaped slot structure is designed on a semi-flexible material in this paper. This arrowhead-shaped slot not only enhances the bandwidth of an antenna but also improves the gain with respect to the reference antenna. The impedance bandwidth of the proposed antenna is 95.93 GHz (3.1-99.17GHz) with a peak gain of 6.91 dBi. The proposed antenna has a fractional bandwidth of 187% with a high Bandwidth Dimension Ratio (BDR) of 3049 with a very compact physical dimension of 22 × 28 × 0.508 mm^3. It has been noted that the proposed antenna gives a very wide bandwidth with a size reduction of 50 % when compared with a conventional circular radiator with respect to lower resonant frequency. The proposed antenna is designed, and the performance analysis has been done using the CST-EM software package in terms of the antenna's different parameters, including impedance bandwidth characteristics, radiation patterns, antenna's gain, radiation efficiency, bending analysis, and the group delay evaluation. The proposed antenna compactness is also theoretically verified with the help of fundamental dimension limit theorem. The proposed antenna has astounding performance because of the wide band range with a very compact size without any adverse effect of bending. This makes the proposed antenna an excellent choice for 5G and Wearable IoT Applications.

II. SWB Antenna Configuration

The proposed arrowhead slot Super Wide Band (SWB) antenna is illustrated in Fig.1 and the detail dimensions of antenna have been depicted in Table I. Antenna is designed on RT Duroid substrate having a relative permittivity of 2.2, loss tangent 0.0009, and thickness of 0.508mm. The overall dimensions of the substrate are *Ws* x *Ls* mm^2. The optimized design parameters of the proposed UWB antenna have been depicted in Table I.

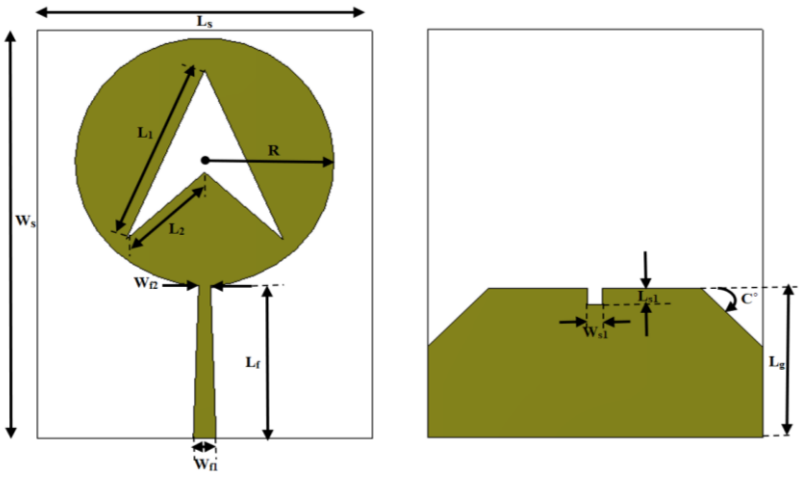

Fig. 1. Arrowhead slot Super Wide Band (SWB) antenna.

The bandwidth of an antenna is directly proportional to the thickness of the substrate and inversely proportional to the square root of substrate thickness [28]. The radius of the circular patch antenna is calculated using (1) which corresponds to VSWR= 2 [29], [30].

ISSN 2179-1074

$$f_L = \frac{7.2}{(L_g + R + p)} GHz \quad (1)$$

The proposed antenna geometry consists of a circular radiating patch with radius 'R' along with the arrowhead slot as shown in Fig.1. The parametric study of the designed patch antenna is carried out in terms of radius, partial ground plane length, slot dimensions, and arrow slot dimensions of the patch antenna. Fig. 2 shows the parametric analysis monopole antenna shown in Fig. 1 concerning partial ground plane and radius of patch antenna. However, the design has evolved from the conventional circular monopole antenna to a final arrowhead slot structure SWB antenna as shown in Fig. 3 (a) to Fig. 3 (e).

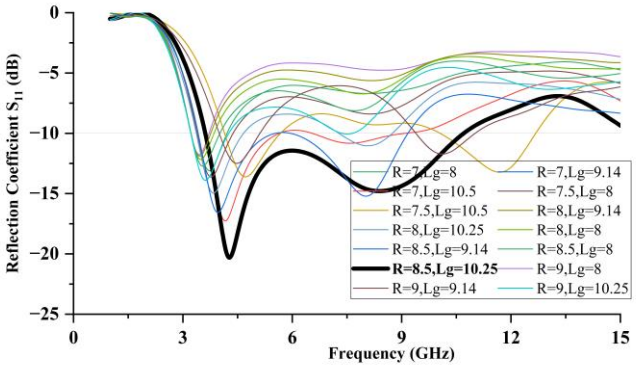

Fig. 2. Parametric analysis of the radius of the patch antenna and length of the ground plane

TABLE I. PARAMETERS OF THE PROPOSED SWB ANTENNA

Parameters	**Dimensions (mm)**	**Parameters**	**Dimensions (mm)**	**Parameters**	**Dimensions (mm)**
Substrate Width (W_S)	22	Chamfering Angle C	45˚	Feed Width (W_{f1})	0.7
Substrate Length (L_S)	28	Feed Width (W_{f1})	1.5	Feed Width (W_{f2})	1.5
Ground Plane Length (Lg)	10.25	Slot Length (L_{s1})	1	Length (L1)	12
Radius of Patch (R)	8.5	Slot width (W_{s1})	1	Length (L2)	7
Feed Length (L_f)	10.5	Chamfering Angle C	45˚	Antenna Height (h)	0.508

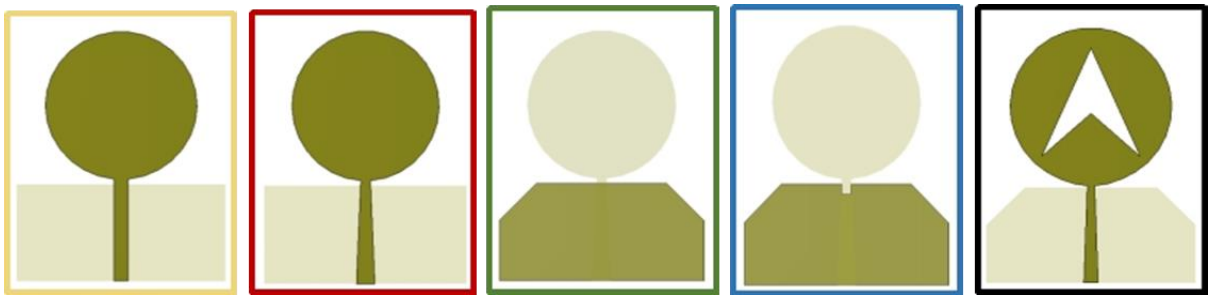

(a) **(b)** **(c)** **(d)** **(e)**

Fig. 3. Arrowhead slot Super Wide Band (SWB) antenna design stage-wise.

The antenna design consists of five stages which include a monopole antenna with rectangular feed, tapered feed region, chamfering, rectangular DGS structure in the ground, and modification in

ISSN 2179-1074

the patch section. The antenna design in Fig. 3 (a) starts with a simple circular monopole antenna as it's a basic technique to get wide and ultra bandwidth and the antenna resonates from 3.49 to 11.95 GHz with an impedance bandwidth of 8.45GHz. Further, an impedance bandwidth of 18.16 GHz i.e. 52.62% more than the first stage using a tapered feed line as shown in Fig. 3 (b) is achieved. The circular monopole antenna with a tapered feed line resonates from 3.38 to 21.5 GHz and it provides good impedance matching. In stage three the chamfering technique has been employed as per Fig. 3 (c) and makes the antenna resonate from 3.01 to 31.61 GHz with an enhanced bandwidth of 36.30% as compared to stage two. The rectangular DGS structure is inserted in the ground plane as in Fig. 3 (d) which added the inductive effect hence neutralizing the capacitive effect and the antenna becomes more resistive and hence increases the impedance bandwidth by 56.88 % (3.03 to 69.17 GHz) as compared to previous stage. Finally, the arrowhead structure shown in Fig. 3 (e) is taken out from the circular patch antenna as it increases the current density in the patch so improves the bandwidth by 31.18% as compared with the previous stage and the antenna resonates from 3.14 to 99.24 GHz with an impedance bandwidth of 96.1 GHz as shown in Fig. 4.

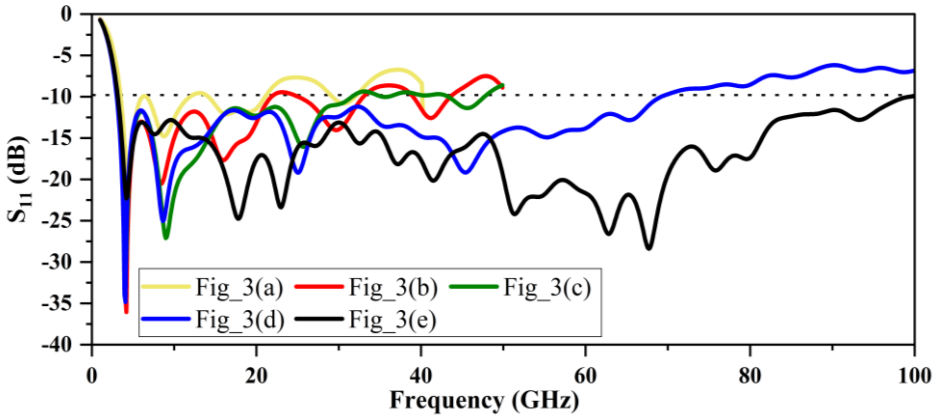

Fig. 4. Simulated return losses of the antenna concerning stage-wise modification.

Table II shows bandwidth enhancement compared to the previous stage design along with the percentage bandwidth achieved in each stage. It has been also noticed that after the implication of each designing stage, the peak gain has also increased. The total gain was enhanced by 3.41 dBi compared to the first stage. The gain of the antenna concerning the entire operating band for different stages is as shown in Fig. 5.

TABLE II. PERCENTAGE BANDWIDTH COMPARISONS OF DIFFERENT STAGES

Stage	Techniques	Frequency range (GHz)	Bandwidth (GHz)	% Increase	% Bandwidth	Peak Gain(dB)
Stage –I	Monopole Antenna with Rectangular Feed line	3.49 to 11.95	8.45	-	109.5	3.51
Stage –II	Monopole antenna using Tapered feed	3.38 to 21.5	18.16	52.62%	145%	5.16
Stage –III	Antenna using Chamfered ground plane	3.01 to 31.61	28.51	36.30%	165%	6.11
Stage –IV	Antenna using chamfered and slot	3.03 to 69.17	66.13	56.88%	183%	6.74
Stage –V	Final Design	3.14 to 99.24	96.1	31.18%	187%	6.92

ISSN 2179-1074

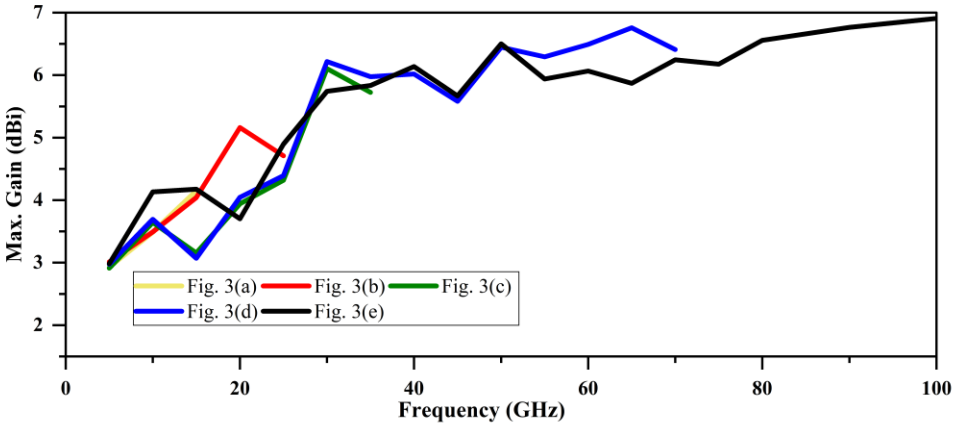

Fig. 5. Gain vs. Frequency plot with respect to stage wise modification.

In order to calculate the overall size reduction, the proposed antenna is compared with a conventional circular radiator with respect to lower resonant frequency. The proposed antenna gives a very wide bandwidth with a size reduction of 50 % as shown in Table III. The overall size reduction makes the proposed antenna compact.

TABLE III. SIZE COMPARISONS WITH A CONVENTIONAL CIRCULAR RADIATOR

Frequency	**Conventional circular radiator size mm^3**	**Proposed SWB antenna radiator size mm^3**	**% Size reduction**
3.1 GHz	620.68	312.92	50%

III. SWB ANTENNA CLOSE TO THE FUNDAMENTAL DIMENSION LIMIT THEORY

Typically an electrically small antenna or compact antenna can be described in terms of the antenna's radian length, $\ell = \lambda/2\pi$ and highest dimension, a. Considering the wavenumber of the electromagnetic wave is represented by, $k = 2\pi/\lambda$, an electrically small antenna can be defined to have the (2)-(3) inequality.

$$a \leq \frac{\lambda}{2\pi} \leq \frac{1}{k} \tag{2}$$

$$ka \leq 1 \tag{3}$$

In other way, a small antenna is one which fits inside a sphere of radius a =1/k. Its greatest dimension is typically less than λ/4 [31], [32].

The inequality between the antenna's electrical size and bandwidth is demonstrated by the quality factor Q. The quality factor Q is defined as the angular frequency ω times the ratio of the reactive energy stored about the antenna to the radiated power. Hence the Q is mathematically expressed as (4) [31].

ISSN 2179-1074

$$Q = \begin{cases} \dfrac{2wW_{Ee}}{\mathrm{P}_{radiated}}, W_{Ee} \geq W_{Me} \\ \dfrac{2wW_{Me}}{\mathrm{P}_{radiated}}, W_{Me} \geq W_{Ee} \end{cases} \tag{4}$$

Where '*w*' denotes the angular frequency, 'W_{Ee}' is the time average, non-propagating stored electric energy, and 'W_{Me}'is the time average, non-propagating stored magnetic energy. The radiated power has been denoted by '$P_{radiated}$'. If the value of Q is high, it is equivalent to the reciprocal of the fractional bandwidth of the antenna as shown in (5). On the other hand, if the antenna Q value is low, the input impedance of the antenna varies slowly with frequency and the antenna has the potential to have a broad bandwidth.

$$Bandwidth = \frac{f_{upper} - f_{lower}}{f_{center}} = \frac{1}{Q} \tag{5}$$

L.J. Chu's developed the expression [33] for quality factor Q for the lowest TM mode is given as below in (6). This equation implies that the value of Q increases rapidly as size decreases and this rapport imposes a critical trade-off between bandwidth and size for an electrically small antenna.

$$Q \cong \frac{1}{k^3 a^3} \tag{6}$$

Further McLean developed a new methodology for the calculation of minimum radiation Q for an antenna. This technique [34], in contrast to Chu's methodology, provides an accurate equation for Q calculation. McLean's and Chu's equations are similar for higher values of the Q equation. However, the two hypotheses disagree for lower values of Q. McLean's expression for quality factor Q is shown in (7).

$$Q = \frac{1}{k^3 a^3} + \frac{1}{ka} \tag{7}$$

The traditional fundamental theories are mostly applicable to the design of narrowband antennas as these theories are based on the consideration of wavenumber for the center frequency of the operating band of the antenna. Wave number is represented by equation (8) [31]:

$$k_L = \frac{2\pi}{\lambda c} \tag{8}$$

However, in the case of UWB/SWB antennas, the wavelength of the center frequency is very different from the lower and upper bound wavelengths, and hence it is not feasible for these antennas to use the concept of utilizing the central wavelength directly for the whole range of frequencies. The appropriate solution is to define the antenna's electrical size to satisfy the equation, k_L stands for the wave number corresponding to the lower bound of the occupied bandwidth [31]. Table IV presents the product *(ka)* of this wave number *(k*) and the antenna sphere radius (*a*) for all the designed and

received 27 Sep 2023; for review 11 Dec 2023; accepted 23 May 2024

ISSN 2179-1074

fabricated SWB antennas proposed in this work. Fig. 6 shows the comparative analysis of proposed SWB antennas (simulated and fabricated) with the Chu and McLean curves. The quality factor Q is plotted with respect to ka.

TABLE IV. ELECTRICAL SIZE CALCULATION OF THE PROPOSED SWB ANTENNA

Approach	Patch Height (mm)	f_L (GHz)	Wavelength at λ_L	Wavenumber (k_L)	k_L*a (rad)
Simulated	0.035	3.12	96.15	0.0653	0.94
Fabricated	0.035	3.16	94.93	0.0661	0.96

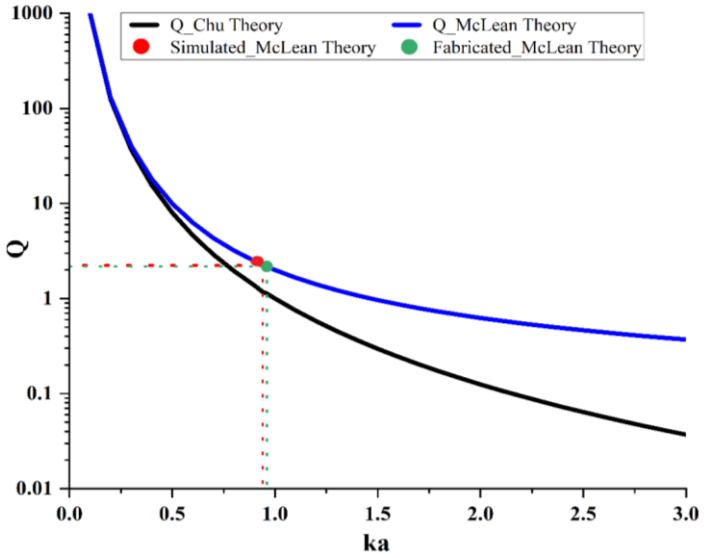

Fig. 6. Comparative analysis of proposed SWB antennas with the Chu and McLean curves.

The quality factor of the proposed SWB antenna is determined using McLean's expression. It has been observed that the proposed SWB antenna agreed well with the McLean's curve of the fundamental dimension limit theory [33], [34] and hence it can be stated that the proposed SWB antenna is designed to get very close to the fundamental limitation theory.

IV. BENDING OR CONFORMAL ANALYSIS

Nowadays, the demand for flexible wireless systems is increasing exponentially due to their diverse applications in several wireless devices in daily life, such as health monitoring, patient diagnosis, telemedicine, and defence applications. Flexible electronic devices play a very important role in IoT applications. Wearable flexible devices are becoming an important part of the next generation of communication systems and Internet of Things (IoT) applications. The most significant component of a wearable flexible device is an antenna. Flexible antennas have been widely employed for on-body and off-body communication [35]. However, when using antennas on curved surfaces, they undergo bending or flexing, which may change the reflection characteristics of antennas. Although the antennas are designed on substrates that are flexible, the designed antennas need to be analyzed with respect to bending to validate the antenna's behaviour in different bending scenarios. The proposed antenna uses an RT Duroid substrate, which is semi-flexible, so its performance has been examined

ISSN 2179-1074

using different bending angles from 0˚,60˚, 90˚, and 120˚, as shown in Fig. 7 (a), Fig. 7 (b), Fig. 7 (c), and Fig. 7 (d) respectively. The performance of an antenna bending in terms of the S_{11} parameter is as shown in Fig. 8.

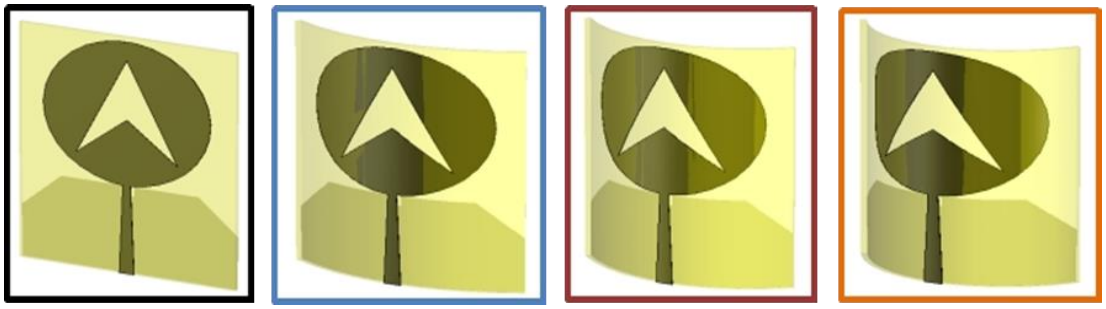

(a) (b) (c) (d)

Fig. 7. Proposed antenna with (a) 0˚ (b) 60˚ (c) 90˚ (d) 120˚ bending angles.

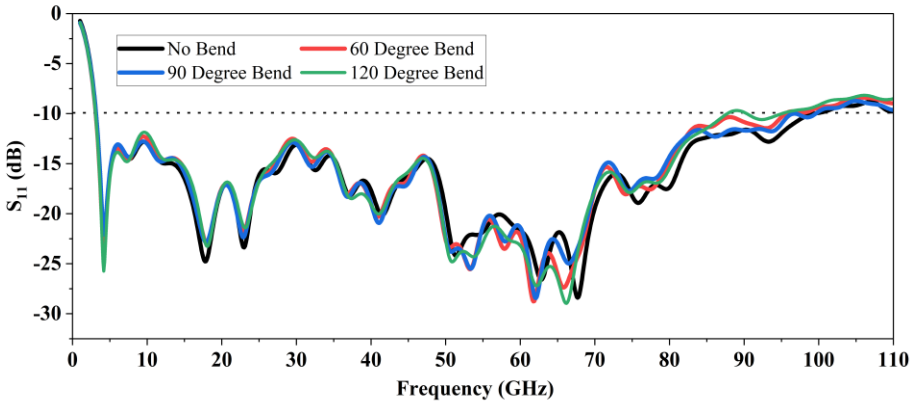

Fig. 8. Proposed antenna reflection coefficient characteristics for bending angles.

It shows a very slight effect on higher frequencies as it has been observed that the higher frequency slightly shifts toward the lower side as the bending angle increases. The proposed antenna's total efficiency for the operating frequency band is shown in Fig. 9. The efficiency varies between 85 to 95% for the mentioned bending angles.

Furthermore, Fig. 10 shows the gain with respect to frequency graph, and it has been observed that for no bending condition, the gain is nearly constant at higher frequencies, but for different bending angles, the gain is slightly more variable, and the peak gain is enhanced as compared to the no-bending condition. The parameters of an antenna are almost the same for all bending angles with slight fluctuations. As the bending is performed on the antenna, its effective length of the patch increases, which affects the overall performance of an antenna [36].

ISSN 2179-1074

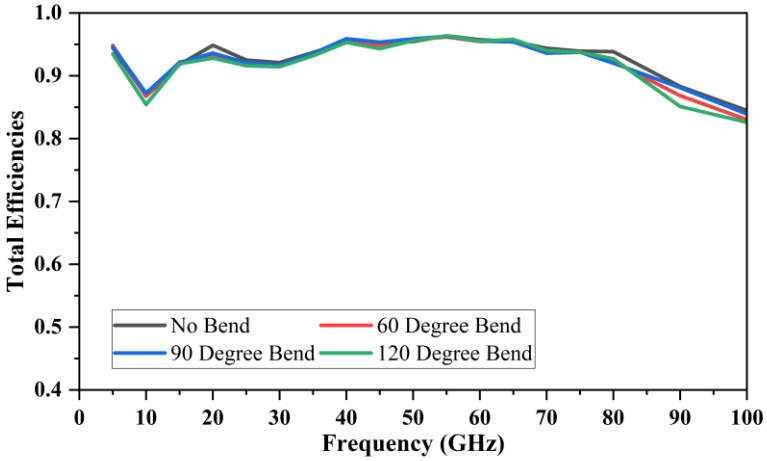

Fig. 9. Total efficiency Vs. Operating Frequency band.

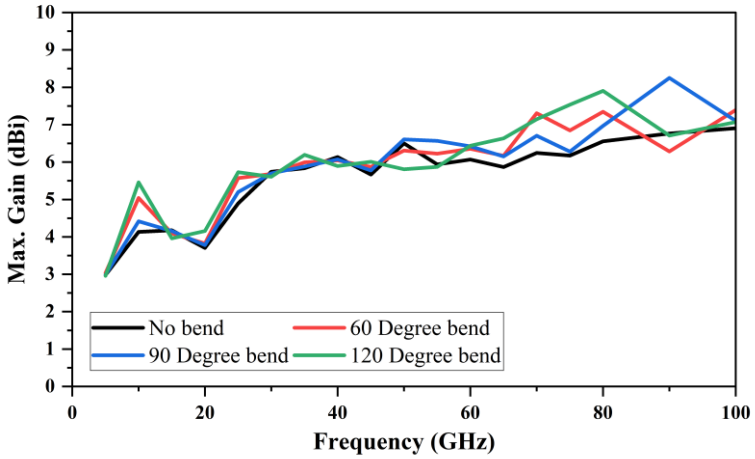

Fig. 10. Gain vs. Operating Frequency band for bending scenario.

V. TIME RESPONSE ANALYSIS

In order to analyze antenna pulse shaping properties, time domain analysis has been performed in this section. The fidelity factor, the phase response of S_{21} and group delay is investigated using time domain analysis. To investigate the time domain response, the two identical antennas, one as a transmitter and another as a receiver antenna, are placed three times λ from each other, i.e., 291 mm from each other. The proposed antennas are placed in face-to-face and side-to-side configurations as shown in Fig.11.

The important time domain characteristics such as fidelity factor, group delay, and phase of S_{21} have been investigated in the following sub section to evaluate the time domain performance of the proposed SWB antenna.

ISSN 2179-1074

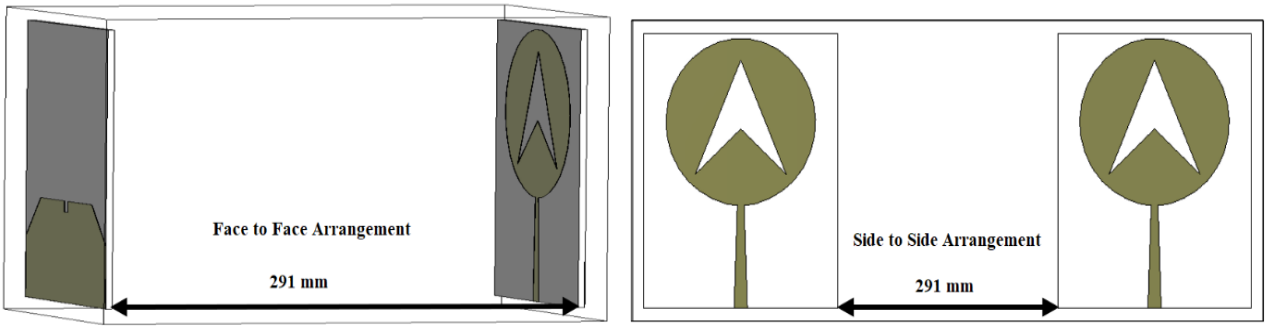

Fig. 11. Antenna Face-to-Face Arrangement and Side-to-Side Arrangement.

A. Fidelity Factor

The equation of fidelity factor in (9) is normalized cross correlation between the Gaussian source pulse and the received pulse, which plays a very important role in minimizing the distortion in the received signal [37].

$$F = \left\{ \frac{\int_{-\infty}^{+\infty} P_t(t) P_r(t-\tau) dt}{\int_{-\infty}^{+\infty} P_t(t)^2 dt . \int_{-\infty}^{+\infty} P_r(t)^2 dt} \right\} \tag{9}$$

Here, P_t (t) is the transmitted or excited signal, P_r(t) is the received signal, and τ is the time delay between both signals. Antennas are placed at a 291mm distance apart, which is three times the wavelength of the lowest operating frequency (3.1 GHz) as shown in Fig. 10. in face-to-face and side-to-side configuration. Because Pr (t) is expected to be much lower than Pt (t), normalization is used to compare only the shape of the signals rather than their magnitude.

Fig. 12 (a) and Fig. 12 (b) show the transmitted and received pulse for both the configurations of the antenna respectively. The fidelity factor has been calculated using Matlab and the fidelity factor obtained for side-by-side and face-to-face configurations are 0.806 and 0.782 respectively. It shows the minimum distortion in signal and received pulse is 80.6 %, and 78.2% similar to the transmitted pulse in the side-by-side and face-to-face configurations respectively.

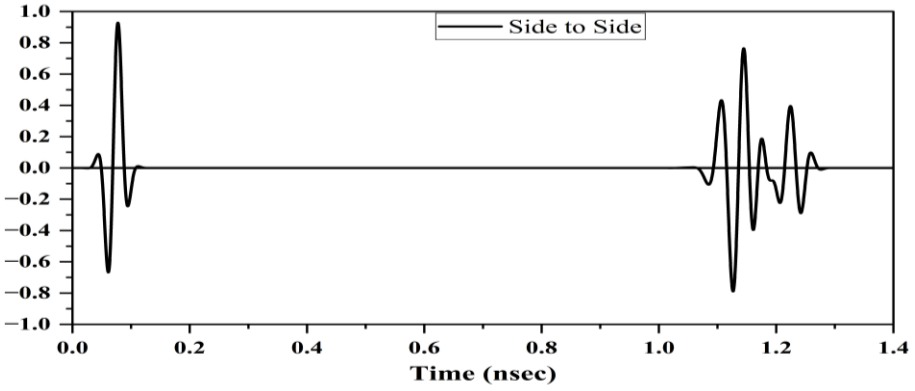

(a)

ISSN 2179-1074

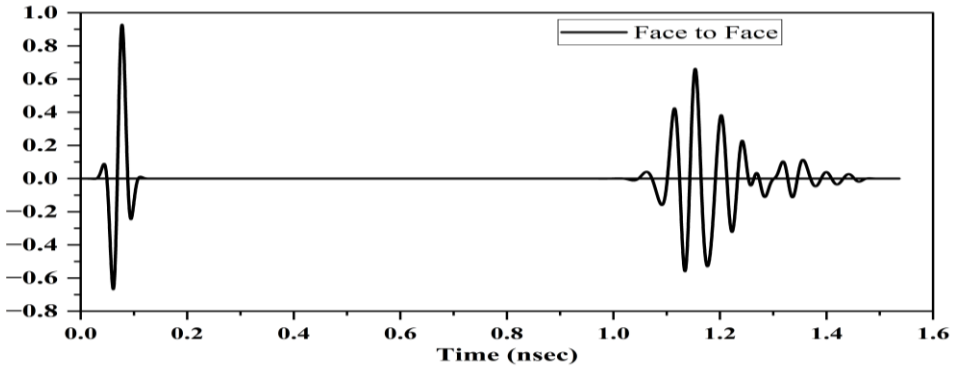

(b)

Fig. 12. Transmitted and Received Signal of Antenna (a) side by side (b) face to face.

B. Group Delay

The phase deviation between the transmitted signal P_t and the received signal P_r is evaluated using Group delay. The time required for a signal to travel from the transmitter antenna to the receiver antenna is calculated as an average group delay. It is calculated using the formula as the negative derivative of phase response with respect to angular frequency [8] and is specified using (10). It is an important parameter of the SWB antenna which calculates the signal delay and total phase distortion of the antenna system [37].

$$\tau_g = -\frac{d\phi(\omega)}{d\omega} = -\frac{1}{2\pi}\frac{d\phi(f)}{df} \tag{10}$$

Where *ϕ(f) represents* the frequency-dependent phase response of the transmitted signal and ω represents the frequency in radians per second. The group delay varies for the side-to-side configuration of the antenna is 1.1 to 1.2 nsec and for the face-to-face configuration varies from 0.7 to 1.1 nsec, which is almost constant group delay as shown in Fig. 13 respectively. The deviation in group delay should be less than the threshold value, i.e., 2 nsec [10], otherwise, phases are non-linear, and it will cause distortion. An ideal antenna should have an antenna transmission coefficient that is usually nearly flat and less than 30dB, and whose phase response shows linearity with respect to frequency. So, it has constant group delay and linear phase response over the entire frequency band. As shown in Fig. 14 the magnitude of S_{21} is less than 30dB for both the configurations face-to-face and side-to-side. Fig. 15 (a) show the phase response over the entire frequency band in side to side configuration and Fig. 15 (b) in face to face configuration, both the cases shows the linear response and this linear phase response ensures the transmission of pulses with minimal distortion. The minimal distortion and nearly constant group delay with less than 1 nsec variations accomplish the requirements of the SWB antenna in time domain response.

ISSN 2179-1074

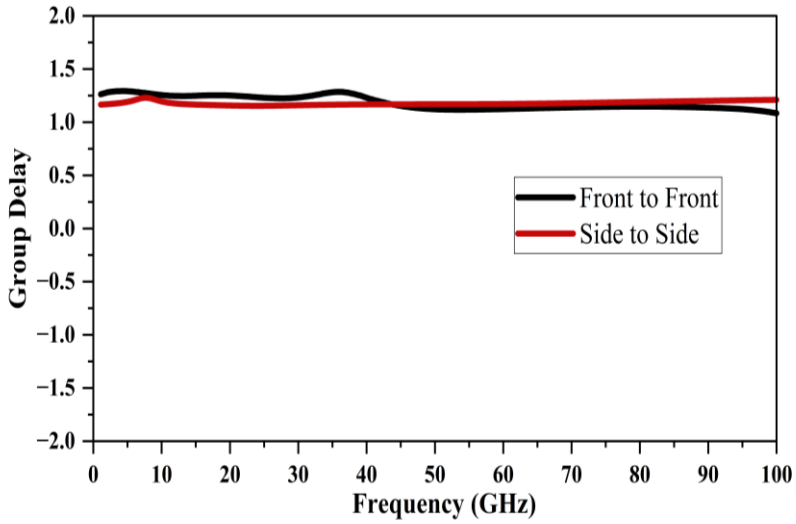

Fig. 13. Group Delay of Side to side and Face to Face configuration respectively.

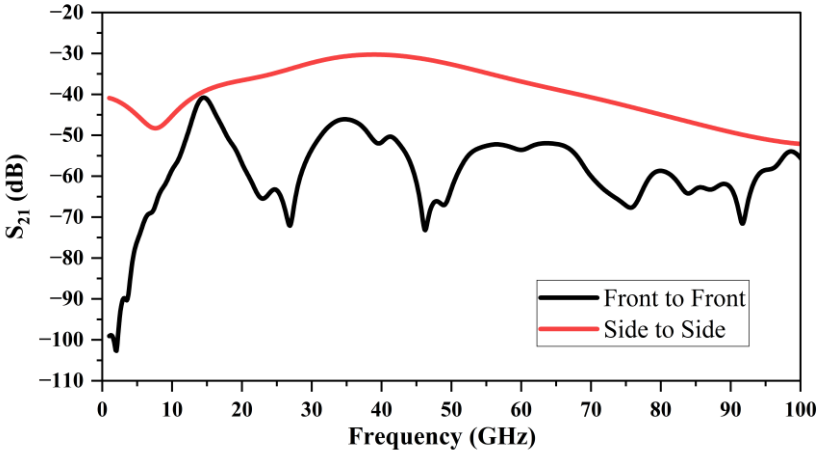

Fig. 14. Magnitude of S_{21} in degrees of Side to side and Face to Face configuration respectively.

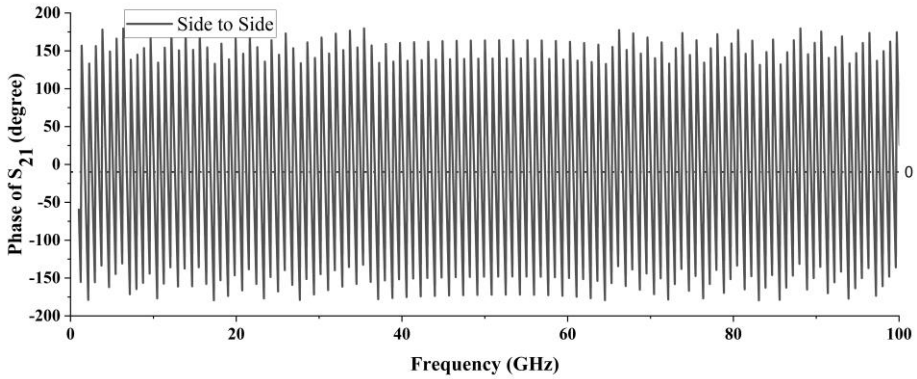

(a)

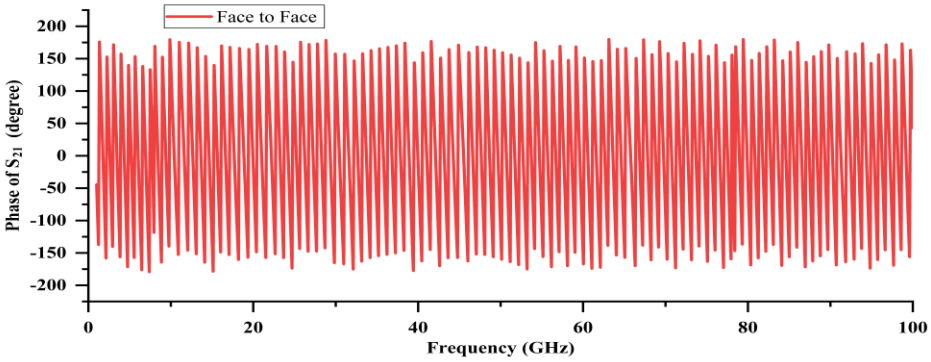

(b)

Fig. 15. Phase of S_{21} in dB of (a) Side to side and (b) Face to Face configuration respectively.

Further to compare the proposed work with the available literature, the proposed SWB antenna is compared with few flexible antennas available in the literature. The comparison is as shown in Table V. The proposed flexible SWB antenna has been compared in terms of size, percentage of bandwidth, bending analysis, fundamental dimension theory analysis, time domain analysis, and peak gain with most of the available flexible SWB-based antennas and a few UWB antennas in the literature, as shown in Table V.

TABLE V. COMPARATIVE ANALYSIS OF THE PROPOSED SWB ANTENNA WITH FEW FLEXIBLE ANTENNAS AVAILABLE IN OPEN LITERATURE

Ref. No.	Antenna Dimension (mm^3)	Frequency Range GHz	Bandwidth %	Peak Gain dBi	Material Used	Bending Analysis	Fundamental Dimension Theory Analysis	Time Domain Analysis
[10]	39 x 45x0.8	2.31 - 40	188.45	5.81	RT Duroid	No	No	Yes
[17]	35 × 30 × 0.8	2.8–40	173.8	7.16	RT Duroid	No	Yes	Yes
[24]	60 x 40x0.1	1.96 to 67	188	9.24	Ultralam 3850	No	No	No
[38]	60x80x2.5	1.4 to 20	173	7.5	Polyester nonwoven fabric	No	No	No
[39]	60 x40x 1	7 to 28	114	NA	flannel.	No	No	No
[40]	34x 25x0.13	1.66 to 56.1	188	6	PET Paper	No	No	Yes
[41]	30x25x0.8	3.1 to 11.5	114	5.25	RT Duroid	Yes	No	Yes
[42]	25 x 25	2.9 to 11.6	118	5.47	Jeans	No	No	Yes
[43]	24.5×22.4 ×1.5	3.1 to 10.7	110	5.9	Cotton	No	No	No
[44]	42.5 × 30 × 0.6	3.25 to 13	120	6.7	Teflon	Yes	No	No
[45]	28 x 30 x 1	2.37- 38.95	177	9	FR4	No	No	No
Proposed	28 x 22 x 0.508	3.12 to 99.6	187	6.9	RT Duroid	Yes	Yes	Yes

The proposed antenna has been compared concerning size with the mentioned reference antennas, and it can be stated that the proposed antenna is the most compact and flexible compared

ISSN 2179-1074

with the size of other antennas concerning its resonating frequency range. The peak gain of the proposed antenna is on the higher side as compared to the reference [39]–[44]. However, the proposed antenna has less gain compared to [24], [38], [17], [45] though the antenna proposed by these references has a very large size and no other analysis has been performed on the antenna. It has been also noted that even though all the antennas mentioned in the comparison table are flexible, still only [41], [44] performed the bending analysis and [40]–[42], [10] performed the time domain analysis

It has been observed that the proposed semi-flexible SWB antenna has a better bandwidth, higher gain, and proves the fundamental dimension limitation theory for compactness. The compactness and better performance characteristics of the proposed flexible SWB antenna in terms of size, bandwidth, flexibility, and group delay, make the proposed antenna most suitable for various wearable IOT applications and medical applications.

VI. Measured Results and Discussion

The proposed SWB antenna has been modelled and designed using 3D Electromagnetic Software; CST (Computer Simulation Technology) based on Finite Integration Technique (FIT).

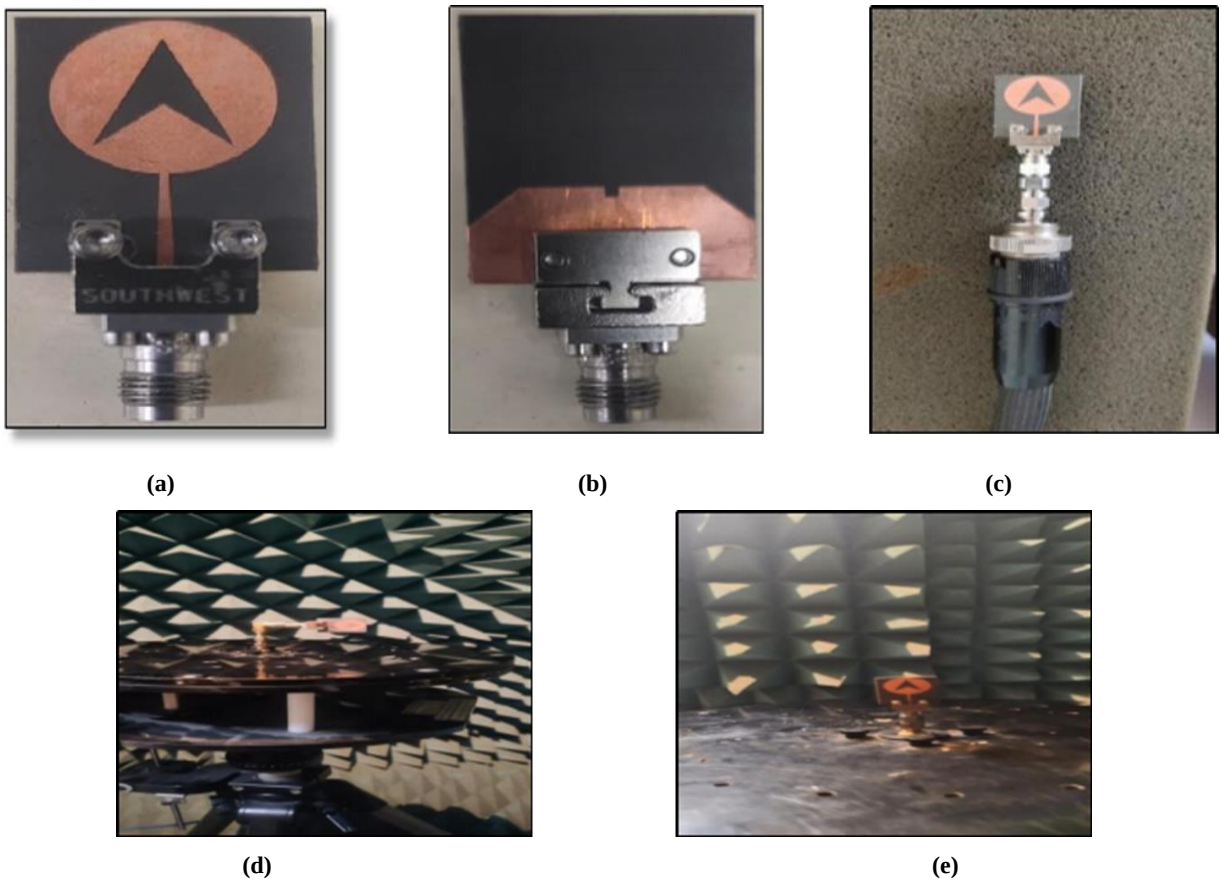

Fig. 16. Fabricated Patch antenna (a) Front side (b) back side (c) VNA setup of SWB Antenna (d,e) Setup of antenna in an anechoic chamber.

The antenna is fabricated on RT Duroid substrate as shown in Fig. 16 (a), Fig. 16 (b), and Fig.16 (c) and used with measurement test setup is as shown in Fig.16 (d) and 16 (e).The reflection coefficient

ISSN 2179-1074

(S_{11}) is tested using the N5227A PNA network analyzer at IIT Delhi up to 60 GHz and the radiation patterns have been measured inside the anechoic chamber with an Antenna Measurement System.

A. *Reflection Coefficient (S_{11}) Characteristics.*

Fig. 17 shows the comparison of the proposed SWB antenna simulated reflection coefficients (S_{11}) with the measured reflection coefficients. The proposed antenna resonates from 3.1 to 99.17GHz. The fabricated antenna has been tested using the N5227A PNA network analyzer with a range of up to 60 GHz only. There is close agreement between simulated and measurement results. However, the slight difference occurs due to the fabrication tolerance error.

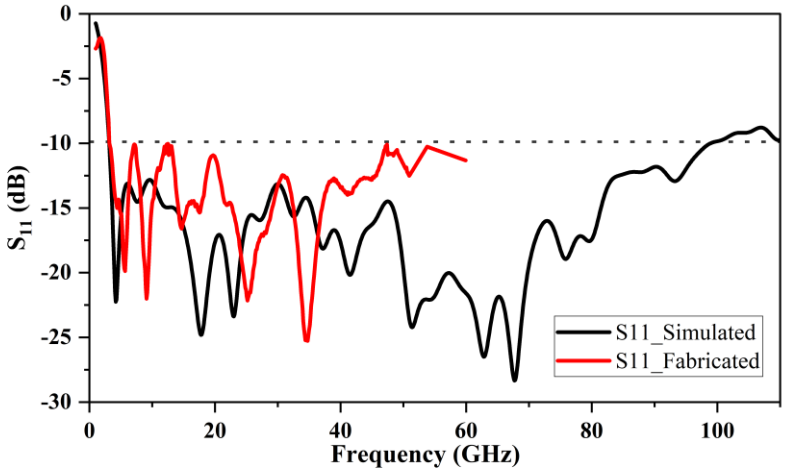

Fig. 17. The return loss versus frequency graph for simulated and measured antenna.

B. Peak Gain

The comparison of simulated and measured gain of a proposed SWB antenna is shown in Fig. 18. The antenna has a gain range of 3 to 6.76 dBi according to the simulated plot and 2.5 to 5.34 dBi according to the measurement results, as shown in Fig. 18. The measured gain pattern is closely followed by the simulated gain.

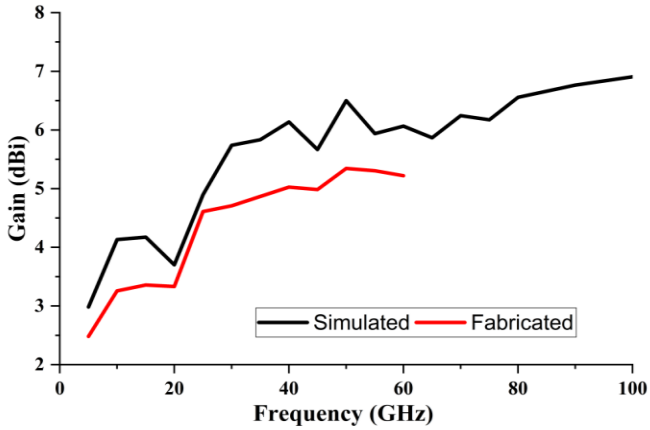

Fig. 18. The variation of gain with frequency for simulated and measured antenna.

ISSN 2179-1074

The variation in gain in the measured pattern is due to connector loss, cable loss, and fabrication error in the fabricated antenna prototype. The gain variation over the entire bandwidth is 2dBi, and the major variation is in the range of 20 to 25GHz, where it is high, and from the frequency range of 25 GHz to 60 GHz, the gain variation is nearly constant, i.e., 0.5dBi.

C. Radiation Patterns

Fig. 18 shows the simulated and measured 2D radiation pattern of the proposed compact SWB antenna in E-plane and H-plane for co and cross-polarized radiated field. Fig. 19 (a), Fig. 19 (b), Fig. 19 (c), and Fig. 19 (d) show the bidirectional radiation pattern for frequencies 5GHz and 10GHz, for simulated E-Co polarized wave and nearby, followed by the measured radiation pattern for the same frequencies and slightly disturbed at higher frequencies. Fig. 19 (e), Fig. 19 (f), Fig. 19 (g), and Fig. 19 (h) show the co-polarized wave in the H-plane and it shows an omnidirectional radiation pattern at lower frequencies such as 5GHz and 10GHz and slightly disturbed at higher frequencies.

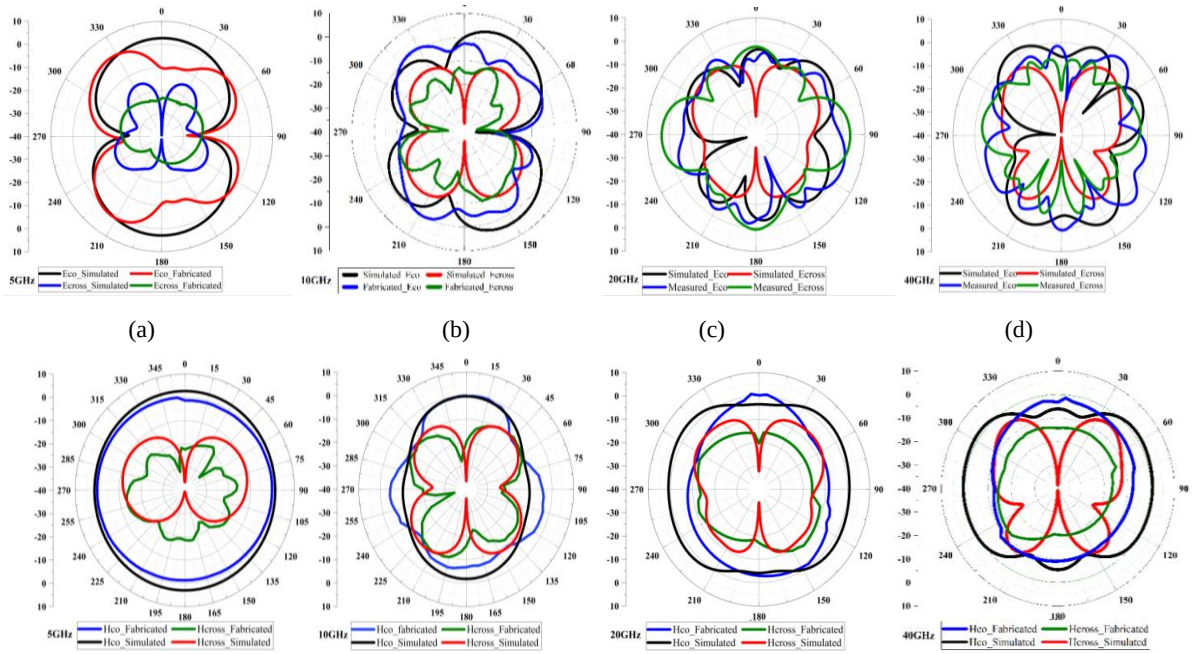

(a) (b) (c) (d)

(e) (f) (g) (h)

Fig. 19. Comparison plot of Simulated and Measured Radiation Patterns E-plane (a) 5GHz (b) 10GHz (c) 20GHz (d) 40 GHz and H-plane (e) 5GHz (f) 10GHz (g) 20GHz (h) 40 GHz.

The disturbance in radiation pattern for H-plane and E-plane patterns is due to higher modes appearing at higher frequency bands. Cross-polarized waves have a magnitude of 20 to 30 dB less than the co-polarized waves and are distinguished from co-polarized waves as expected in measured as well as simulated radiation patterns.

VII. CONCLUSION

In this work, a compact, semi-flexible, arrowhead slot SWB antenna is designed and analyzed for 5G and wearable IoT applications. The impedance bandwidth of 95.93GHz (3.1-99.17GHz) with a peak gain of 6.91 dBi has been achieved for a very compact physical dimension of 22 x 28 x 0.508 mm^3

ISSN 2179-1074

using the tapered feed technique, chamfering, DGS structure in the ground, and an inventive modification in patch section. The proposed antenna is suitable for super wideband applications with a fractional bandwidth of 187% and a bandwidth dimension ratio (BDR) of 3049. In order to prove the relevance of the proposed antenna for wearable IoT applications, the compactness is theoretically verified with the help of the fundamental dimension limit theorem. In addition to this, the flexibility and bending capabilities of materials are also tested under different bending conditions. Additionally, the minimal distortion and nearly constant group delay with less than 1 nsec variations accomplish the requirements of the SWB antenna in time domain response. The proposed antenna also covers the whole high frequency spectrum while maintaining good gain and efficiency, which makes the proposed antenna not only suitable for wearable IoT applications but also for 5G communication systems.

REFERENCES

[1] T. S. Rappaport, Y. Xing, G. R. MacCartney, A. F. Molisch, E. Mellios, and J. Zhang, "Overview of Millimeter Wave Communications for Fifth-Generation (5G) Wireless Networks—With a Focus on Propagation Models," *IEEE Transactions on Antennas and Propagation*, vol. 65, no. 12, pp. 6213–6230, 2017, doi: 10.1109/TAP.2017.2734243.

[2] "5G Network Uses Nearly Same Frequency as Weaponized Crowd Control Systems RF (Radio Frequency) Safe," *Available: https://www.rfsafe.com/5g-network-uses-nearlysame-frequency-as-weaponized-crowd-control-systems.*

[3] "5G Frequency Bands & Spectrum Allocations," *CableFree*, 2019.

[4] L. Camargos, "WRC-19 strikes a good balance, sets stage for mmWave 5G," *GSMA*, 2019.

[5] M. U. Ali Khan, R. Raad, F. Tubbal, P. I. Theoharis, S. Liu, and J. Foroughi, "Bending Analysis of Polymer-Based Flexible Antennas for Wearable, General IoT Applications: A Review," *Polymers (Basel)*, vol. 13, no. 3, p. 357, 2021, doi: 10.3390/polym13030357.

[6] W. Yu, W. Li, D.-C. Chang, and Y. Li, "Small Antennas: Miniaturization Techniques and Applications," *International Journal of Antennas and Propagation*, vol. 2014, pp. 1–1, 2014, doi: 10.1155/2014/134103.

[7] R. A. Pandhare, M. P. Abegaonkar, and C. Dhote, "UWB antenna with novel FSS reflector for the enhancement of the gain and bandwidth", *International Journal of Microwave and Wireless Technologies*, vol. 14, no. 10, pp. 1353–1368, 2022, doi: 10.1017/S1759078721001781.

[8] W. Balani *et al.*, "Design Techniques of Super-Wideband Antenna–Existing and Future Prospective," *IEEE Access*, vol. 7, pp. 141241–141257, 2019, doi: 10.1109/ACCESS.2019.2943655.

[9] S. K. Palaniswamy, M. Kanagasabai, S. Arun Kumar, M. G. N. Alsath, S. Velan, and J. K. Pakkathillam, "Super wideband printed monopole antenna for ultra wideband applications," *International Journal of Microwave and Wireless Technologies*, vol. 9, no. 1, pp. 133–141, 2017, doi: 10.1017/S1759078715000951.

[10] V. Sharma, Gunaram, J. K. Deegwal, and D. Mathur, "Super-Wideband Compact Offset Elliptical Ring Patch Antenna for 5G Applications," *Wireless Personal Communications*, vol. 122, no. 2, 2022, doi: 10.1007/s11277-021-08965-4.

[11] H. R. D. Oskouei, A. R. Dastkhosh, A. Mirtaheri, and M. Naseh, "A Small Cost-Effective Super Ultra-Wideband Microstrip Antenna with Variable Band-Notch Filtering and Improved Radiation Pattern with 5G/Iot Applications," *Progress In Electromagnetics Research M*, vol. 83, pp. 191–202, 2019, doi: 10.2528/PIERM19051802.

[12] S. Alluri and N. Rangaswamy, "Compact high bandwidth dimension ratio steering-shaped super wideband antenna for future wireless communication applications" *Microwave and Optical Technology Letters*, vol. 62, no. 12, pp. 3985–3991, 2020, doi: 10.1002/mop.32541.

[13] V. Dhasarathan, M. Sharma, M. Kapil, P. C. Vashist, S. K. Patel, and T. K. Nguyen, "Integrated bluetooth/LTE2600 superwideband monopole antenna with triple notched (WiMAX/WLAN/DSS) band characteristics for UWB/X/Ku band wireless network applications" *Wireless Networks*, vol. 26, no. 4, pp. 2845–2855, 2020, doi: 10.1007/s11276-019-02230-0.

[14] M. Elhabchi, M. N. Srifi, and R. Touahni, "A novel modified U-shaped microstrip antenna for super wide band (SWB) applications," *Analog Integrated Circuits and Signal Processing*, vol. 102, no. 3, pp. 571–578, 2020, doi: 10.1007/s10470-020-01589-x.

[15] A. Gorai, A. Karmakar, M. Pal, and R. Ghatak, "A CPW-Fed Propeller Shaped Monopole Antenna with Super Wideband Characteristics" *Progress In Electromagnetics Research C*, vol. 45, pp. 125–135, 2013, doi: 10.2528/PIERC13082805.

[16] R. Azim, M. T. Islam, H. Arshad, Md. M. Alam, N. Sobahi, and A. I. Khan, "CPW-Fed Super-Wideband Antenna With Modified Vertical Bow-Tie-Shaped Patch for Wireless Sensor Networks," *IEEE Access*, vol. 9, pp. 5343–5353, 2021, doi: 10.1109/ACCESS.2020.3048052.

received 27 Sep 2023; for review 11 Dec 2023; accepted 23 May 2024

ISSN 2179-1074

[17] S. Kundu and A. Chatterjee, "A compact super wideband antenna with stable and improved radiation using super wideband frequency selective surface," *AEU - International Journal of Electronics and Communications*, vol. 150, p. 154200, 2022, doi: 10.1016/j.aeue.2022.154200.

[18] S. Kundu, "Experimental study of a printed ultra-wideband modified circular monopole antenna" *Microwave and Optical Technology Letters*, vol. 61, no. 5, pp. 1388–1393, 2019, doi: 10.1002/mop.31736.

[19] B. L. Shahu, S. Pal, and N. Chattoraj, "Design of super wideband hexagonal-shaped fractal antenna with triangular slot," *Microwave and Optical Technology Letters*, vol. 57, no. 7, pp. 1659–1662, 2015, doi: 10.1002/mop.29184.

[20] Sagne, Dipika, and Rashmi A. Pandhare. "Design and Analysis of Inscribed Fractal Super Wideband Antenna for Microwave Applications." *Progress In Electromagnetics Research C,* 121 ,2022.

[21] S. Das, D. Mitra, and S. R. Bhadra Chaudhuri, "Staircase Fractal Loaded Microstrip Patch Antenna for Super Wide Band Operation," *Progress In Electromagnetics Research C*, vol. 95, pp. 183–194, 2019, doi: 10.2528/PIERC19070105.

[22] Y. H. Peter S. Hall, *Antennas and Propagation for Body-Centric Wireless Communications; Artech House: London, UK, 2012.*, Second Edition. 2012.

[23] R. Lakshmanan and S. K. Sukumaran, "Flexible Ultra Wide Band Antenna for WBAN Applications," *Procedia Technology*, vol. 24, pp. 880–887, 2016, doi: 10.1016/j.protcy.2016.05.149.

[24] S. Dey, M. S. Arefin, and N. C. Karmakar, "Design and Experimental Analysis of a Novel Compact and Flexible Super Wide Band Antenna for 5G," *IEEE Access*, vol. 9, pp. 46698–46708, 2021, doi: 10.1109/ACCESS.2021.3068082.

[25] T. K. Saha, T. N. Knaus, A. Khosla, and P. K. Sekhar, "A CPW-fed flexible UWB antenna for IoT applications," *Microsystem Technologies*, vol. 28, no. 1, pp. 5–11, 2022, doi: 10.1007/s00542-018-4260-0.

[26] M. Tighezza, S. K. A. Rahim, and M. T. Islam, "Flexible wideband antenna for 5G applications," *Microwave and Optical Technology Letters*, vol. 60, no. 1, pp. 38–44, 2018, doi: 10.1002/mop.30906.

[27] A. Al-Sehemi, A. Al-Ghamdi, N. Dishovsky, G. Atanasova, and N. Atanasov, "A flexible broadband antenna for IoT applications," *International Journal of Microwave and Wireless Technologies*, vol. 12, no. 6, pp. 531–540, 2020, doi: 10.1017/S1759078720000161.

[28] C. A. Balanis, *Antenna theory: analysis and design. John wiley & sons,* 2015.

[29] K. P. Ray and Y. Ranga, "Ultrawideband Printed Elliptical Monopole Antennas," *IEEE transactions on antennas and propagation*, vol. 55, no. 4, pp. 1189–1192, 2007, doi: 10.1109/TAP.2007.893408.

[30] K. P. Ray and S. Tiwari, "Ultra wideband printed hexagonal monopole antennas," *IET Microwaves, Antennas & Propagation*, vol. 4, no. 4, p. 437, 2010, doi: 10.1049/iet-map.2008.0201.

[31] S. Dey and N. C. Karmakar, "Design of novel super wide band antenna close to the fundamental dimension limit theory," *Scientific Reports*, vol. 10, no. 1, p. 16306, 2020, doi: 10.1038/s41598-020-73478-2.

[32] M. Ayyappan and P. Patel, "On Design of a Triple Elliptical Super Wideband Antenna for 5G Applications," *IEEE Access*, vol. 10, pp. 76031–76043, 2022, doi: 10.1109/ACCESS.2022.3185241.

[33] L. J. Chu, "Physical Limitations of Omni-Directional Antennas," *Journal of applied physics*, vol. 19, no. 12, pp. 1163–1175, 1948, doi: 10.1063/1.1715038.

[34] J. S. McLean, "A re-examination of the fundamental limits on the radiation Q of electrically small antennas," *IEEE Transactions on antennas and propagation*, vol. 44, no. 5, p. 672, 1996, doi: 10.1109/8.496253.

[35] S. Mohandoss, S. K. Palaniswamy, R. R. Thipparaju, M. Kanagasabai, B. R. Bobbili Naga, and S. Kumar, "On the bending and time domain analysis of compact wideband flexible monopole antennas," *AEU - International Journal of Electronics and Communications*, vol. 101, pp. 168–181, 2019, doi: 10.1016/j.aeue.2019.01.015.

[36] R. Vashi, T. Upadhyaya, and A. Desai, "Graphene-based wide band semi-flexible array antenna with parasitic patch for smart wireless devices," *International Journal of Microwave and Wireless Technologies*, vol. 14, no. 1, pp. 86–94, 2022, doi: 10.1017/S1759078721000179.

[37] S. Singhal, P. Singh, and A. Kumar Singh, "Asymmetrically CPW-fed octagonal sierpinski UWB fractal antenna," *Microwave and optical technology letters*, vol. 58, no. 7, pp. 1738–1745, 2016, doi: 10.1002/mop.29903.

[38] M. Karimyian-Mohammadabadi, M. A. Dorostkar, F. Shokuohi, M. Shanbeh, and A. Torkan, "Super-wideband textile fractal antenna for wireless body area networks," *Journal of electromagnetic waves and applications*, vol. 29, no. 13, pp. 1728–1740, 2015, doi: 10.1080/09205071.2015.1060139.

[39] S. Meghana, G. S. Karthikeya, B. K. Sujatha, and P. Prabhakar, "A Super Wideband Washable Antenna Demonstrated On Flannel," *Progress In Electromagnetics Research Letters*, vol. 102, pp. 95–100, 2022, doi: 10.2528/PIERL21120801.

[40] M. Rabiul Hasan, M. A. Riheen, P. Sekhar, and T. Karacolak, "Compact CPW-fed circular patch flexible antenna for super-wideband applications," *IET Microwaves, Antennas and Propagation*, vol. 14, no. 10, pp. 1069–1073, 2020, doi: 10.1049/iet-map.2020.0155.

[41] B. Prudhvi Nadh, B. T. P. Madhav, M. Siva Kumar, M. Venkateswara Rao, and T. Anilkumar, "Circular ring structured ultra-wideband antenna for wearable applications," *International Journal of RF and Microwave Computer-Aided Engineering*, vol. 29, no. 4, p. e21580, 2019, doi: 10.1002/mmce.21580.

[42] A. Yadav, V. Kumar Singh, A. Kumar Bhoi, G. Marques, B. Garcia-Zapirain, and I. de la Torre Díez, "Wireless Body Area Networks: UWB Wearable Textile Antenna for Telemedicine and Mobile Health Systems," *Micromachines (Basel)*, vol. 11, no. 6, p. 558, May 2020, doi: 10.3390/mi11060558.

[43] B. Tiwari, S. H. Gupta, and V. Balyan, "Design and comparative analysis of compact flexible UWB antenna using different substrate materials for WBAN applications," *Applied Physics A*, vol. 126, no. 11, Nov. 2020, doi: 10.1007/s00339-020-04011-5.

received 27 Sep 2023; for review 11 Dec 2023; accepted 23 May 2024

ISSN 2179-1074

[44] S. Lakrit, S. Das, B. T. P. Madhav, and K. Vasu Babu, “An octagonal star shaped flexible UWB antenna with band-notched characteristics for WLAN applications,” *Journal of Instrumentation*, vol. 15, no. 2, Feb. 2020, doi: 10.1088/1748-0221/15/02/P02021.

[45] A. Kumar, V. Kumar, R. Sharma, and A. P. S. Pharwaha. "On the development of compact super-wideband fractal antenna." *Indian Journal of Science and Technology* 16, no. 15: 1145-1152, 2023.

  ISSN 2179-1074